Improving the birefringence using a graded core photonic crystal fiber

A. SONNE*, A. OUCHAR
Telecommunication, Signal and Systems Laboratory, Electronic Department. University of Laghouat, Algeria

In this paper we report the control of birefringence in octagonal-lattice photonic crystal fiber by doped gradually the central part of the core. Based on our results, the birefringence is found to be largely on the variation of the materials, number of elliptical air holes ring and diameter of the graded core region. The maximal model birefringence of our proposed PCF at the excitation wavelength of $\lambda = 1550$ nm can be achieved 7.12×10^{-3}. The Finite Difference Time Domain with Transparent Boundary Condition is used to analyze such PCF.

(Received April 25, 2014; accepted January 21, 2015)

Keywords: Photonic crystal fiber (PCF), High birefringence, Graded core PCF (GC-PCF), The Finite Difference Time Domain (FDTD), Transparent Boundary Condition (TBC)

1. Introduction

Photonic crystal fibers (PCFs) have created a revolution in the fiber industry as a result of their many extraordinary properties like signal mode operation in wide band, high birefringence, ultra-flattened chromatic dispersion, low confinement loss, large effective mode area [1-10], which cannot be obtained by conventional optical fibers. The conventional PCFs are essentially formed by air holes embedded in silica or another material with a constant refractive index [11-12]. In this paper, a new designed PCF structure is proposed, which is doped gradually in the central part of the core. Among the features of PCFs, birefringence is one of the most interesting characteristics. These highly birefringent PCFs have a great deal potential of practical use in optical communication systems, devices and sensors. High level of birefringence in PCFs is required to maintain the linear polarization state by reducing polarization coupling.

Many methods have been recommended to induce high birefringence PCFs, such as, using different air hole sizes or elliptical air holes in the cladding instead of circular ones [13], squeezing the air holes lattice [14], or using asymmetric core [15]. The control of birefringence in our proposed graded-core PCF (GC-PCF) has been demonstrated by inducing the doped core gradually, by varying diameter core region, by introducing elliptical air holes in the inner rings.

The effect of varying refractive index in the core region and radius of doped region is studied to find the trends of birefringence variation and then applied to the design of highly birefringence PCF. Applying the full-vector finite difference time domain (FDTD) with transparent boundary condition (TBC), the birefringence of the GC-PCF is investigated in detail. The FDTD method that we used is analyzed numerically using Opti-FDTD module of the commercially available Optiwave software [16].

2. Design parameters of GC-PCF

Fig. 1 shows the PCF designs. The two layer cladding (conventional PCF and proposed GC-PCFs) is composed of a common air hole diameter$d = 1.4\ \mu m$, the pitch $\Lambda = 2.3\ \mu$mand $\Lambda_1 = 1.76\ \mu m$, number of rings, elliptical air hole major axis *a* and minor axis *b*, ellipticity $\eta = b/a = 4.6$, the number of elliptical air holes E_{RN} and the arrangement of the holes. In additional the central part of the core in figure 1.b (proposed GC-PCF) is doped gradually with lowest index. In our work, the refractive index of the air hole is $n_0 = 1$, and the refractive index of the cladding is $n = 1.5$.

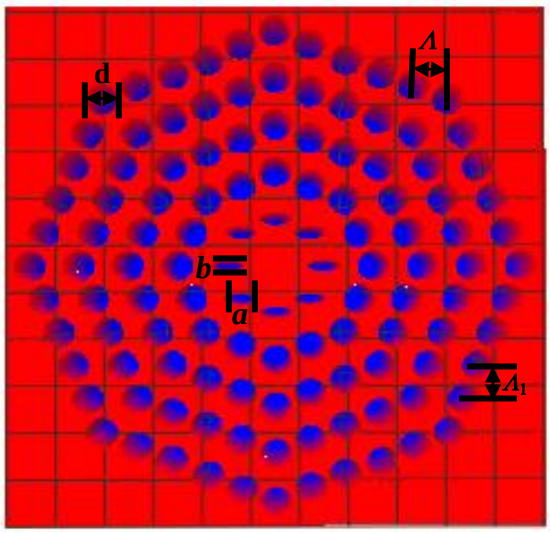

a

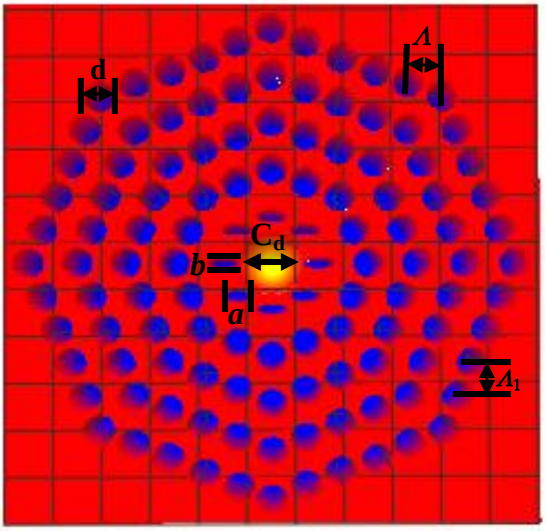

b

Fig. 1. Cross-section of our proposed (a) conventional PCF, (b) GC-PCF with E_{RN}= 1

In order to show the difference in the refractive indices of the core region, the refractive index profile of our proposed conventional and GC-PCFs are shown in Figure 2. The index profile of the core region of our proposed GC-PCF is shown by the following equation:

$$n(\rho) = N_{min}\sqrt{1 - 2\Delta\left(\frac{\rho}{C_d}\right)^{\alpha}} \qquad 0 < \rho < C_d \qquad (1)$$

Where N_{min} is the refractive index of the core center, C_d is the radius of the core, α is the difference of the index profile and Δ is the relative index difference between the core center and the cladding layer defined as:

$$\Delta = \left(N_{min}{}^2 - n_1{}^2\right)/\left(2N_{min}{}^2\right) \qquad (2)$$

In this work we fixed α as 1.5~2 (parabolic profile), then we analyze the birefringence of PCFs versus C_d with different N_{min}. In future studies, we intend to study the changing of α and its effect on the trends of birefringence. From figure 2 (b) it is clear that the refractive index of the core region of our proposed GC-PCF declines gradually from its lowest value N_{min}at the center of the core to a value at the edge of the core that equals the refractive index of the cladding background (n=1.5).

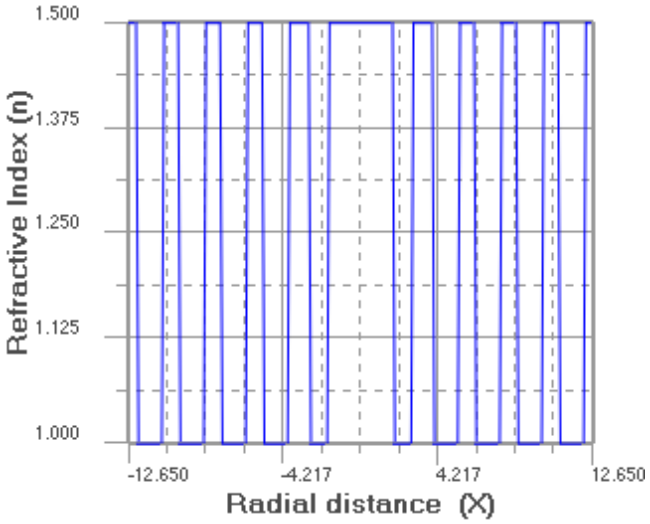

a

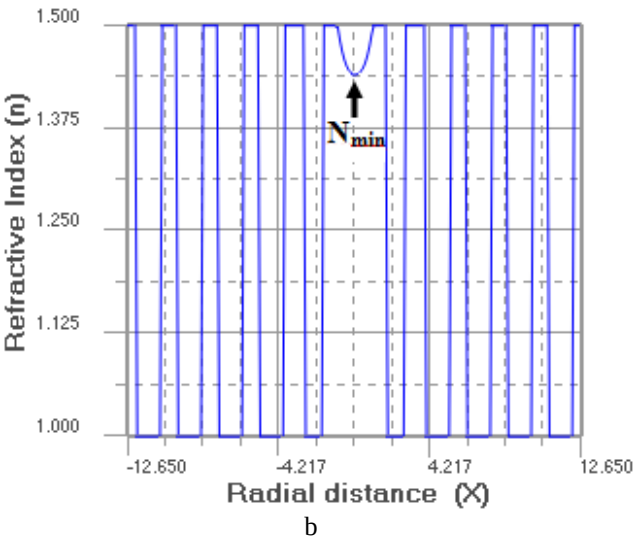

b

Fig. 2. Refractive index profile of our proposed (a) conventional PCF (b) GC-PCFs structures

3. Results and discussion

We calculate the field distribution and effective model index n_{eff} of the designed GC-PCF by using the finite difference time domain (FDTD) method with transparent boundary condition (TBC) [16]. Based on the calculated refractive index properties, the phase birefringence *B*,

defined as the difference between the propagation constants β_x and β_y of the two orthogonal polarized components, is calculated according to the formula [17]:

$$B = n_x - n_y = \frac{\lambda}{2\pi}(\beta_x - \beta_y) \quad (3)$$

Theoretically, introducing more rings of elliptical air holes is more helpful to tailor the properties of PCF such as birefringence [18]. We examine the effect of changing air hole shape from circular to elliptical of the three inner rings on the birefringence of the conventional PCF. Figure 3 shows the absolute value of birefringence as a function of wavelength for the three changing. The curves with the square, circular and triangular symbols represent elliptical air holes in one, two and three inner rings respectively. From this figure, it can be seen that birefringence monotonically increases with increasing wavelength, and the number of elliptical air holes rings affects the birefringence more significantly when in longer wavelength range. However, we found that the difference between conventional PCF with E_{RN} = 1 and 2 is larger than the difference between conventional PCF with E_{RN} = 2 and 3. The conventional PCF with E_{RN} = 1, 2 and 3exhibit birefringence of $2.25 \times 10^{-3}, 2.27 \times 10^{-3}$and 2.85×10^{-3}0 at 1.55 µm, respectively.

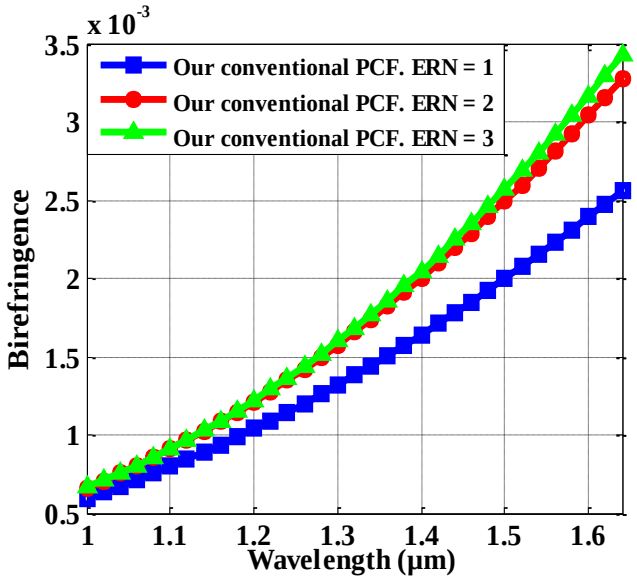

Fig. 3. The birefringence as function of wavelength of conventional PCF with one, two and three elliptical air holes rings

To illustrate typical field distribution of the fundamental mode, we show in Fig. 4 the x-polarized mode for our proposed conventional PCF with E_{RN} = 1 at 1.55 µm. It is shown that the field is concentrated on the center of fiber.

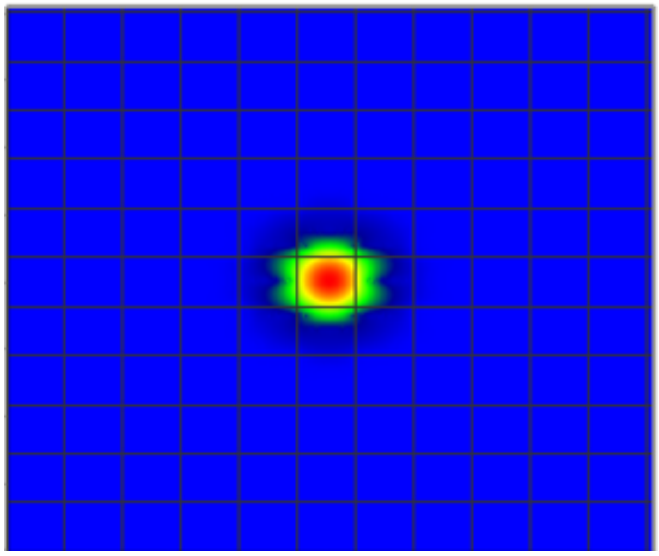

Fig. 4.Mode field distribution in x-polarized of the fundamental mode of our proposed conventional PCF with E_{RN} = 1 at λ=1.55µm

As we all know, the birefringence of the optical fiber is sensitive to the mode field distribution. Fig. 5 (a)-(c) shows the mode field distribution in x-polarized of the fundamental mode of our proposed GC-PCF with different N_{min} when $C_d = 3\ \mu m$ and E_{RN} =1 at $\lambda = 1.55$ µm. It can be observed that the mode filed in the fiber diffuses to the cladding slowly with the decreasing of N_{min}.

Fig. 6 shows the effective index of the x- and y-polarized fundamental mode GC-PCF as a function of wavelength with $N_{min} = 1.48$, $N_{min} = 1.46$ and $N_{min} = 1.44$ at $C_d = 3\mu m$. As seen from figure 6, the index of the x-polarized fundamental mode is larger than that of the y-polarized one, and their difference reaches an order of 10^{-3} at 1550 nm. It can be clearly observed that as N_{min} is decreased, the modal index difference between the two fundamental x- and y- polarized modes increases, and it can also be observed from figure 5 that as N_{min}, is decreased, the mode field will penetrate more into the asymmetrical cladding region. This is due to the fact that with the decreased N_{min}, the equivalent index of the core region is reduced, which increases the index contrast between the effective cladding and the graded core. So, we have concluded that the effect of the modal index difference between the two fundamental x- and y-polarized modes is more obvious if the index contrast between the core-cladding is high.

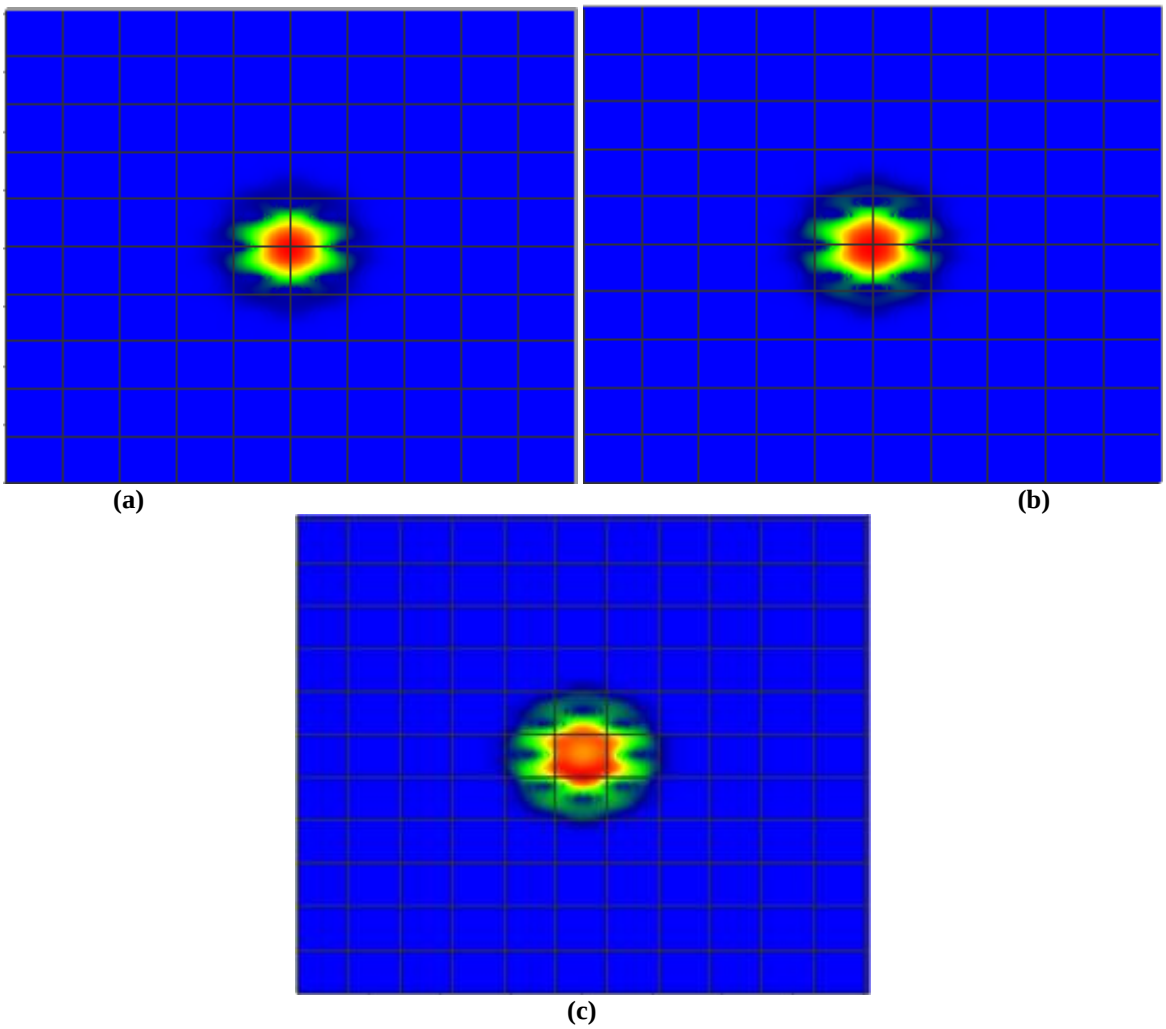

Fig. 5. Mode field distribution in x-polarized of the fundamental mode of our proposed GC-PCF with E_{RN} = 1 at λ=1.55 μm: (a) $N_{min} = 1.48$, (b) $N_{min} = 1.46$, (c) $N_{min} = 1.44$

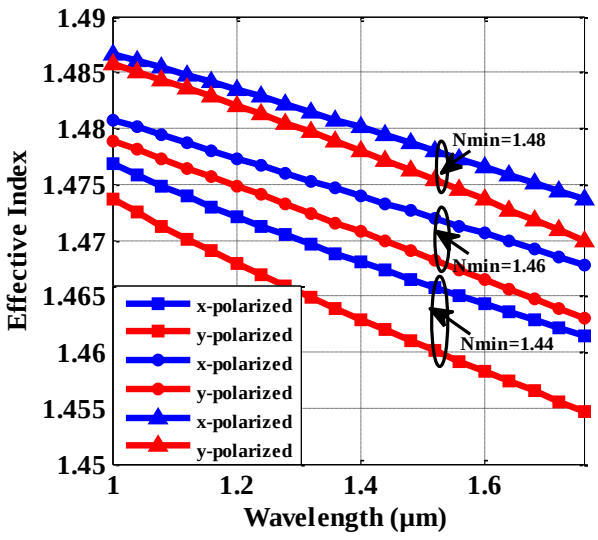

Fig. 6. Effective index of the x- and y-polarized fundamental mode GC-PCF states as a function of wavelength

Fig. 7 shows the birefringence of our proposed GC-PCF with E_{RN}= 1 as a function of core region diameter C_d at excitation wavelength $\lambda = 1.55\ \mu m$. It can be seen that the birefringence is sensitive to the varying refractive index in the core centerN_{min}.

In Fig. 7, we find that the birefringence at 1.55 μm of our proposed GC-PCF is higher than that in previous conventional PCF when the value of C_d is larger than 1 μm whatever was the value of N_{min}. Figure 7 indicates that for each family of curves ($N_{min} = 1.44, 1.45, 1.46, 1.47, 1.48$ and 1.49), the birefringence increases first and then decreases with the increase of the core region diameter C_d, and the maximum value of birefringence occurred at $C_d = 4\ \mu m$ whatever was the value of N_{min}. It can also be noted that for each family of curves, the birefringence increases with the refractive indices of the core center N_{min} decreases, the birefringence values at $C_d = 4\ \mu m$ are found to be 2.75×10^{-3}, 3.45×10^{-3}, 4.3×10^{-3}, 5.25×10^{-3}, 6.18×10^{-3} and 7.02×10^{-3} when the $N_{min}$are 1.49, 1.48, 1.47, 1.46, 1.45 and 1.44 respectively.

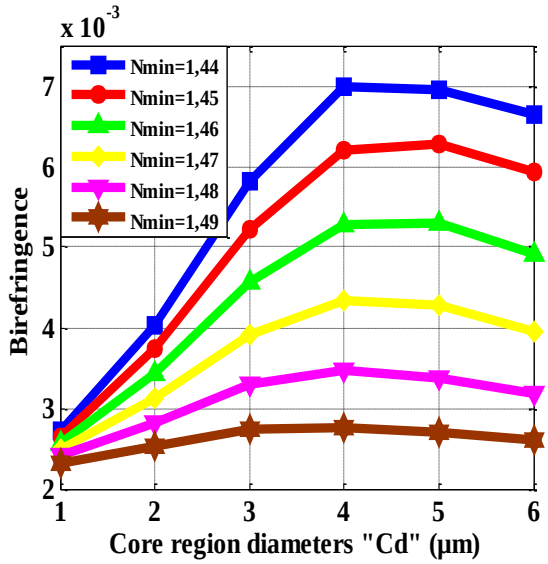

Fig. 7. Modal birefringence versus the parameter Cd for our proposed GC-PCF with E_{RN} = 1 and various N_{min} at 1.55 µm

The birefringence increases with the decreases of N_{min} because the difference in refractive index between the core center N_{min} and the background cladding increases. That is to say, the large difference of refractive index represents a strong perturbation to the field.

In the next step, we proceed to investigate the influence of the number of elliptical air holes rings in our proposed GC-PCF.

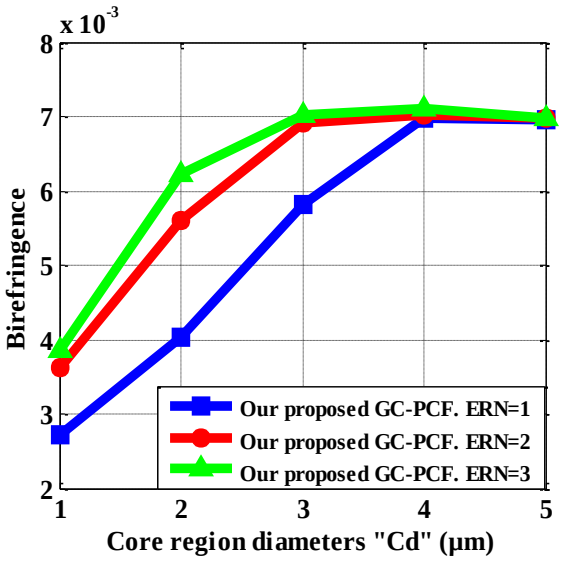

Fig. 8. Modal birefringence versus the parameter C_d for our proposed GC-PCF with E_{RN}=1, 2, 3 and N_{min} = 1.44 at 1.55 µm

Fig. 8 shows the simulation results for the comparison of the birefringence obtained from our proposed GC-PCF as a function of the core region diameter C_d with E_{RN} = 1, 2 and 3 at N_{min} = 1.44. It can be seen that the birefringence is sensitive to the number of elliptical air holes rings, and all the birefringence curves increase with C_d, and reaches a maximum value at $C_d = 4\ \mu m$, after that it gradually decreases. It can also be noted that the birefringence of our proposed GC-PCF with E_{RN} = 3 is higher than that of GC-PCF with E_{RN} = 1 and 2 as the value of C_d is less than 3µm. In addition, it is also observed that the birefringence is almost of the same value between E_{RN}= 2 and 3 and higher than E_{RN} = 1when the value of C_d varies from 3µm to 4µm, and we can also note that all curves (E_{RN} = 1, 2 and 3) are almost of the same value when C_d is larger than 4 µm. For our proposed GC-PCF with E_{RN} = 3, a maximum value of 7.12×10^{-3} is reached at $C_d = 4\ \mu m$, which is clearly that this value is almost the same with E_{RN} = 1 and 2. In this step we have deduced that the increase of E_{RN} strengthen the asymmetric structure of our proposed GC-PCF when the value of C_d is less than 3µm.

Fig. 8 shows the field distribution in x-polarized of the fundamental mode of our proposed GC-PCF with E_{RN} = 1, N_{min} = 1.44 and $C_d = 3\ \mu m$, (a) at λ=0.85µm, (b) λ=1.55µm.

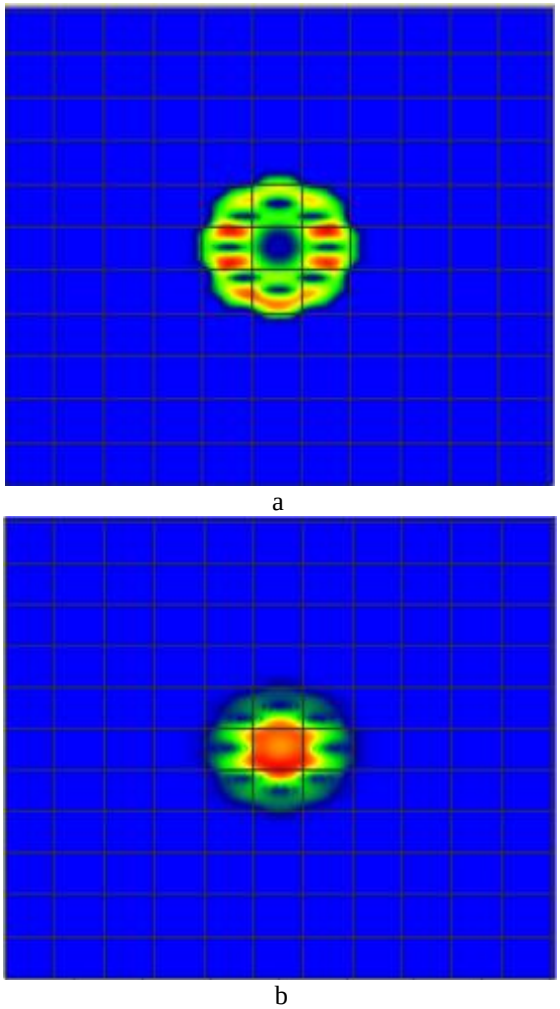

Fig. 9. Mode field distribution in x-polarized of the fundamental mode of our proposed GC-PCF with E_{RN} = 1 and C_d = 3µm; (a) at λ =0.85µm, (b) λ=1.55µm

It can be observed from Fig. 8 that with the wavelength increasing, the modal fields distribution become more concentrated on the center of fiber, which is the opposite distribution of the conventional PCF [18], due to that the center core index is lower than the cladding background. Comparing Fig. 4 with Fig. 9(b), one can see that the maximum of the field of Fig. 9 (b) is concentrated in the center of the core, but the field extends far from the core therefore birefringence increases.

4. Conclusion

In conclusion, we have proposed a GC-PCF with properties similar to that of a proposed conventional PCF. The obtained results (birefringence $B = 7.12 \times 10^{-3}$) show that the birefringence of our proposed GC-PCF is much higher than the proposed conventional PCF (birefringence $B = 2.85 \times 10^{-3}$). It has been found that doping gradually the center core of PCF with low indexes than cladding background shift up the birefringence curve, and the shift is much more significant at the diameter core region $C_d = 4\ \mu m$. The simulation results prove that the increasing of E_{RN} have strong influences of the birefringence when the value of C_d is less than 3µm.

References

[1] R. Sharma, V. Janyani, S.-K. Bhatnagar. J. Mod. Opt. **58**, 604 (2012).
[2] C. Gui, J. Wang, IEEE. Photon. J., **4**, 2152 (2012).
[3] T. Matsui, J. Zhou, K. Nakajima, I. Sankawa, J. Lightwave Technol. **23**, 4178 (2005).
[4] R. Sharma, V. Janyani;, S.K. Bhatnagar J. Mod. Opt., **59**, 205 (2012).
[5] Z. Liu, X. Liu,; S. Li, G. Zhou, W. Wang, L. Hou, Opt. Commun., **272**, 92 (2007)
[6] N. Hai, Y. Namihira, S. Kaijage, F. Begun, S. Abdur Razzak, K. Miyagi, Opt. Rev., **16**, 351 (2009).
[7] J. Liang, M. Yun, W. Kong, X. Sun, W. Zhang, S. Xi, Optik. Opt., **122**, 2151 (2011).
[8] S. Abdur Razzak, Y. Namihira, F. Begun, K. Miyagi, S. Kaijage, N. Hai, T. Kinjo, N. Zou, Opt. Rev. **14**, 165 (2007).
[9] S. Haxha, H. Ademgil, Opt. Commun., **281**, 278 (2008).
[10] N-H. Hai, Y. Namihira, S. Kaijage, T. Kinjo, Opt. Rev. **15**, 91 (2008)
[11] Y.-F. Chau, J. Mod. Opt., **58**, 1673 (2011).
[12] T.-J. Yang, L.-F. Shen, Y.-F. Chau, M.-J. Sung, D. Chen, D.-P. Tsai, Opt. Commun., **281**, 4334 (2008).
[13] Z. Wu, D.-X. Yang, L. Wang, L. Rao, L. Zhang, K. Chen, W.-J. He, S. Liu, Opt. Laser. Technol. **42**, 387 (2010).
[14] F. Beltran-Mejia, G. Chesini, E. Silvestre, Opt. Lett., **32**, 544 (2010).
[15] T.-P. Hansen, J. Broeng, S.-B. Libori, E. Knudsen, A. Bjarklev, J.-R. Jensen, H. Simon-sen, IEEE Photon.Technol. Lett., **13**, 588 (2001).
[16] Technical Background and Tutorial of OPTIFDTD; Optiwave System Inc.; Canada, 2010.
[17] D. Wang, L. Wang, Opt. Commun., **284**, 5568 (2011).
[18] J. Wang, C. Jiang, W. Hu, M. Gao, H. Ren, Opt. Laser.Technol., **39**, 913 (2007).

*Corresponding author: a.sonne@mail.lagh-univ.dz